Arctic Ocean surface warming trends over the past 100 years

Michael Steele,[1] Wendy Ermold,[1] and Jinlun Zhang[1]

Received 10 August 2007; revised 20 November 2007; accepted 5 December 2007; published 29 January 2008.

[1] Ocean temperature profiles and satellite data have been analyzed for summertime sea surface temperature (SST) and upper ocean heat content variations over the past century, with a focus on the Arctic Ocean peripheral seas. We find that many areas cooled up to ~0.5°C per decade during 1930–1965 as the Arctic Oscillation (AO) index generally fell, while these areas warmed during 1965–1995 as the AO index generally rose. Warming is particularly pronounced since 1995, and especially since 2000. Summer 2007 SST anomalies are up to 5°C. The increase in upper ocean summertime warming since 1965 is sufficient to reduce the following winter's ice growth by as much as 0.75 m. Alternatively, this heat may return to the atmosphere before any ice forms, representing a fall freeze-up delay of two weeks to two months. This returned heat might be carried by winds over terrestrial tundra ecosystems, contributing to the local heat budget. **Citation:** Steele, M., W. Ermold, and J. Zhang (2008), Arctic Ocean surface warming trends over the past 100 years, *Geophys. Res. Lett.*, *35*, L02614, doi:10.1029/2007GL031651.

1. Introduction

[2] The Arctic Ocean has been warming over the past few decades [*Polyakov et al.*, 2007; *Zhang*, 2005]. Most attention in this regard has focused on pulses of relatively warm water from the North Atlantic Ocean, which enter the Arctic Ocean in two streams from the Nordic Seas [*Gerdes et al.*, 2003; *Schauer et al.*, 2002]. These waters eventually subduct beneath colder, fresher surface waters that originate from a combination of river runoff and Pacific Ocean sources [*Steele and Boyd*, 1998]. Thus most studies, observational and modeling, have focused on the warming of this sub-surface layer residing at depths of 150–800 m within much of the Arctic Ocean.

[3] But what about the surface waters? The arctic sea ice cover is also changing, with September sea ice extent shrinking since 1979 at a rate of 9% per decade [*Serreze et al.*, 2007]. Within the Arctic Ocean, the reduction has occurred mainly in the marginal seas of the Alaskan and Russian continental shelves. This creates a longer season in which the ice cover is absent and surface atmospheric fluxes (particularly shortwave radiation) might warm the ocean above the freezing point. At the same time, there is evidence of increasing heat entering the Arctic Ocean through Bering Strait [*Woodgate et al.*, 2006] and possibly melting sea ice [*Shimada et al.*, 2006] since this water typically resides at depths just below the mixed layer (~40 m) down to ~150 m [*Steele et al.*, 2004]. In this study we examine historical trends in summertime heating of the upper layers of the arctic seas using in situ temperature profiles and satellite data.

2. Data

[4] We use July, August, and September ("summer") ocean temperature profiles from the World Ocean Database (WOD'05) [*Johnson et al.*, 2006] over the domain 60–90°N, which includes the Nordic Seas, Arctic Ocean, Canadian arctic waters, and the northern edge of the Bering Sea (Figure 1a). These summer data number 240,851 profiles over the years 1805–2005, representing 41% of the total annual data over our domain. For the six Arctic Ocean shelf seas specially marked in Figure 1, 43% of the data are from summer and 88% of these summer data are from 1930 and later. Relatively few post-1995 observations exist on the Russian arctic shelves.

[5] We consider here two diagnostics of upper ocean heat content: sea surface temperature (SST) and upper ocean heat content (OHC). SST is defined here as the mean temperature over the upper 10 m, since many profiles do not start right at 0 m depth. About 9% of the original profiles were discarded for the SST calculation because their shallowest data lie below 10 m depth. OHC is defined here as the integrated ocean heat content relative to −2°C, from the surface to 100 m depth or the ocean bottom, whichever is shallower. For OHC, a profile must contain data within layers at the top and bottom that are 10% of the thickness of the total integration distance (e.g., 10 m for a 100 m integration). This criterion, which eliminated 24% of the original profiles, ensures that the data reasonably span the total integration interval.

[6] For each year, the data were averaged into 50 km bins to reduce spatial bias (Figure 1), and thereafter were regarded as the input data for further analyses. These input data were discarded if their SSTs were greater than three standard deviations away from the climatological mean SSTs spanning 1950–1989 as defined by *Steele et al.* [2001], which eliminated 0.7% of the input data. Since this climatological mean might differ slightly from the longer record WOD'05 mean, the remaining input data were averaged into 400 km bins and a further 0.4% were discarded as greater than three standard deviations away from these means.

[7] Trends were then computed on a 200 km grid by simple linear regression of a running 3-year mean of the input data within overlapping 400 km bins, and then further smoothed by a running 500 km Hanning filter. For each year, a summer mean was only calculated if there were at least four 50 km input data in each 3-year period in each 400 km bin. Trends were calculated only if there were at least three years of input data over the regression period,

[1]Polar Science Center, Applied Physics Laboratory, University of Washington, Seattle, Washington, USA.

0094-8276/08/2007GL031651$05.00

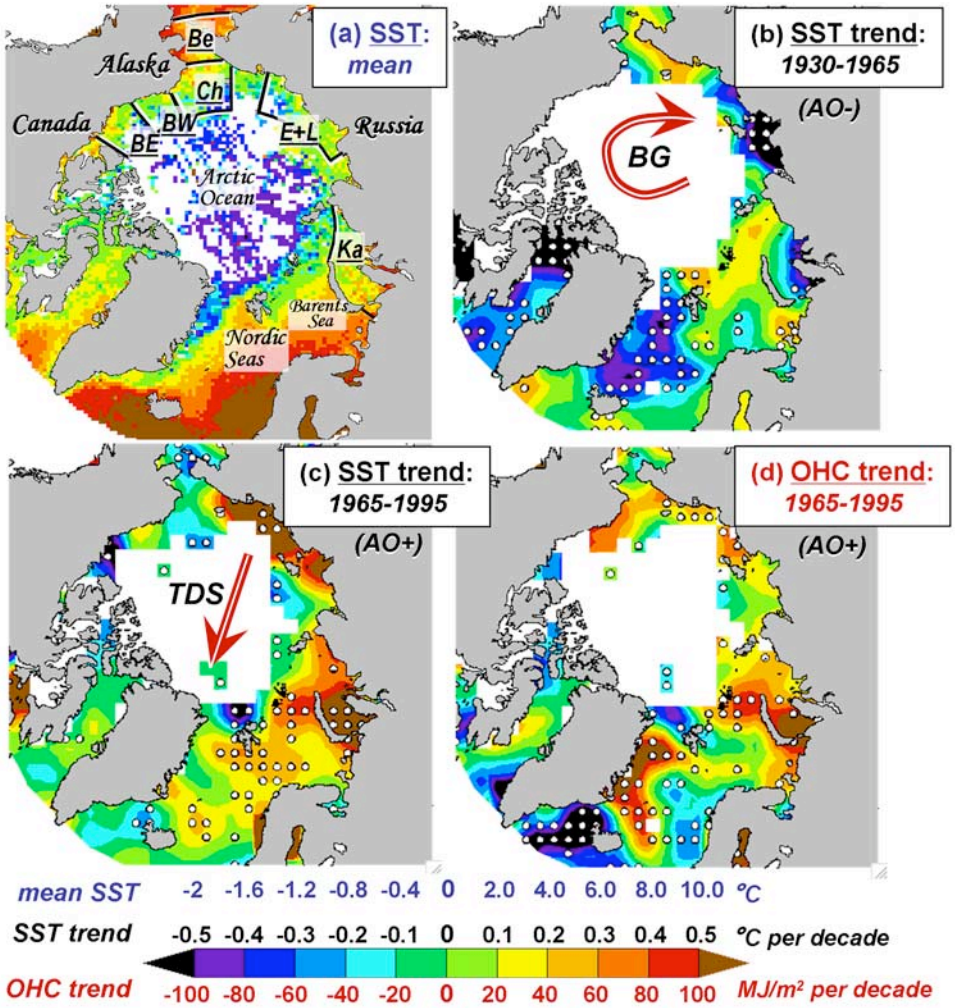

Figure 1. (a) Mean summer temperature distribution over 1805–2005 in the World Ocean Database [*Johnson et al.*, 2006] averaged into 50 km bins within the upper 10 m. Selected shelf seas are BE = eastern Beaufort Sea, BW = western Beaufort Sea, Ch = Chukchi Sea, Be = Bering Sea, E + L = western East Siberian plus eastern Laptev Seas, and Ka = Kara Sea. The next two panels show linear summer SST trends using in situ WOD'05 data over (b) 1930–1965 and (c) 1965–1995. Red arrows indicate sea ice drift patterns, i.e., the Beaufort Gyre (BG) and Transpolar Drift Stream (TDS). Also shown are (d) summer OHC trends over 1965–1995. Dots indicate 95% significance; the number of significant bins in all trend maps exceed the minimum threshold for statistical field significance [*Livezey and Chen*, 1983] by at least 9%.

and only if there were input data within ±3 years of both the start and end dates.

[8] For regional trends over the arctic shelves defined in Figure 1, a multiple regression in both space and time was performed in order to reduce spatial sampling bias, with linear predictors x, y, t, and a mean SST climatology [*Steele et al.*, 2001]. This last predictor allows for curvature in the predicted spatial field [*Steele and Ermold*, 2004]. A minimum of three input data were required in each year to form a summer mean. Similar results (not shown) were obtained when a linear predictor in depth was added to the SST multiple regression. An intra-seasonal time variable was not used, as it has been found to degrade the analysis of such sparse data [*Steele and Ermold*, 2004].

[9] Regional SST trends were extended through summer 2007 using a blended satellite and in situ monthly mean data set with 1 degree latitude and longitude resolution [*Reynolds et al.*, 2002], which we averaged into annual summer means. A mean bias and root-mean-square (RMS) difference between the WOD'05 data and the satellite data were computed for each region, using data from all overlap years, starting in 1982 (the first year of satellite data). Biases were 0.2°C–0.8°C, similar to those found in the North Atlantic Ocean [*Kumar et al.*, 2003], while RMS differences were 0.8°C–1.4°C, similar to the relatively large values found by *Reynolds et al.* [2002] in the data-sparse arctic seas.

3. Results

[10] Figure 1b shows a map of the linear trend in summer SST anomalies over the years 1930–1965, a period during which the North Atlantic Oscillation and Arctic Oscillation indices both generally declined [*Ostermeier and Wallace*, 2003] and thus referred to hereafter as "AO–." Figure 1c shows a similar map for the years 1965–1995, when these climate indices generally rose, hereafter referred to as

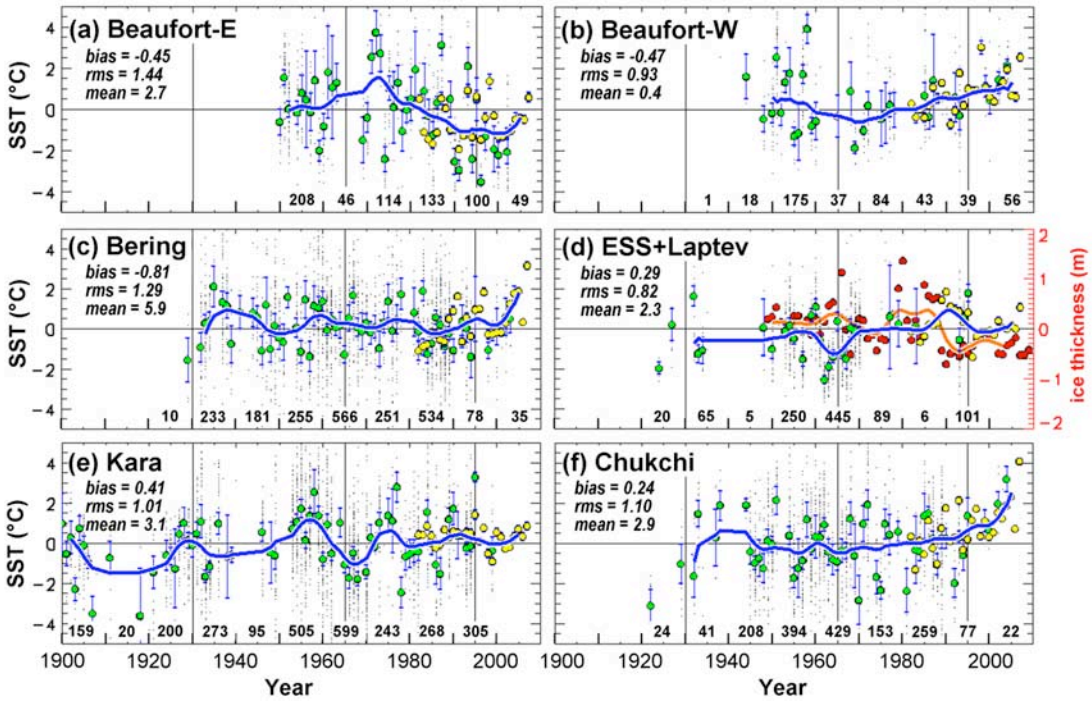

Figure 2. Mean summer SST anomalies for the six shelf regions defined in Figure 1a. Shown are the 50 km binned in situ input anomalies (gray dots), the regional means of these anomalies (green dots), 95% confidence range of these means (i.e., ±1.96 standard errors, vertical blue lines), and number of 50 km bins with in situ data in each decade (along the bottom axis of each panel). Also shown are the summer-mean satellite-derived SSTs (yellow dots) adjusted by the mean difference over the data record (i.e., bias) of the in situ summer means minus the satellite means. The bias and rms difference are noted in each panel. Smoothed regional means (blue curves) are computed from the average in each summer of the green and yellow dots by application of a 3-year running median filter followed by 2 passes of a 5-year running mean filter. Anomalies were computed relative to the mean spatial fields for 1965–1995, and the mean value over each region during this time period is noted in each panel. Vertical black lines indicate the periods 1930–1965 (i.e., "AO−") and 1965–1995 (i.e., "AO+"). The red dots in Figure 2d show mean springtime (March–April–May) ice thickness in the ESS + Laptev region from the model of *Zhang and Rothrock* [2003], while the orange curve takes these red dots and smoothes them in the same manner as for SST.

"AO+." Trends are generally weaker over the total period 1930–1995 (not shown). OHC trends over the AO+ period are shown in Figure 1d. The AO− and AO+ periods have been shown to produce distinct trends in Arctic Ocean shelf salinity [*Steele and Ermold*, 2004] and river discharge trends [*Peterson et al.*, 2002] over 1930–1995, although both older and more recent arctic geophysical time seres are not as tightly controlled by this forcing [e.g., *Polyakova et al.*, 2006; *Rigor and Wallace*, 2004; *Stroeve et al.*, 2006].

[11] The Nordic Seas generally cooled during AO− and warmed during AO+ [e.g., *Dickson et al.*, 1996]. A similar behavior is evident in the southern Kara Sea, where warming trends during AO+ are clearly stronger than those upstream in the Barents Sea. This might indicate a local heating source from river discharge or elsewhere, or an advancing intrusion of warm Atlantic Waters that only in AO+ years reach the southern Kara Sea [*Zhang et al.*, 1998].

[12] The western East Siberian and eastern Laptev Seas (hereafter, "ESS + Laptev Seas") also cool during AO− and warm during AO+, possibly owing to sea ice conditions tied to the Arctic Oscillation. *Belchansky et al.* [2004] show that for the period 1979–2001, ESS melt onset is earlier and freeze-up is later during AO+ years. Given an increasing AO index trend over 1965–1995, this implies a lengthening open water season and thus more solar heating of the upper ocean. Summertime ocean heating might also occur via sensible heat transfer from stronger southerly winds [*Maslanik et al.*, 1996]. On the other hand, advection of warm Pacific Waters is an unlikely heat source for this region during AO+, as *Semiletov et al.* [2005] shows a retreat of these waters from this region in these years.

[13] Why does sea ice retreat from the ESS earlier in the year during AO+? One potential mechanism is the enhanced warm southerly winds discussed by *Maslanik et al.* [1996], which both melt ice and blow it away from the coast. On the other hand, *Francis and Hunter* [2006] indicate a strong contribution from downwelling longwave radiation. Finally, *Zhang et al.* [2000] noted in a model study that the reduced Beaufort Gyre associated with AO+ reduces the convergence of sea ice into the ESS. Thus AO+ ESS sea ice should be thinner at the start of the melt season simply because of weaker advection from the western Arctic Ocean and stronger advection away from the shelf as the Transpolar Drift Stream shifts cyclonically in these years [*Proshutinsky and Johnson*, 1997; *Steele and Boyd*, 1998]. These shifts are illustrated in Figures 1b and 1c.

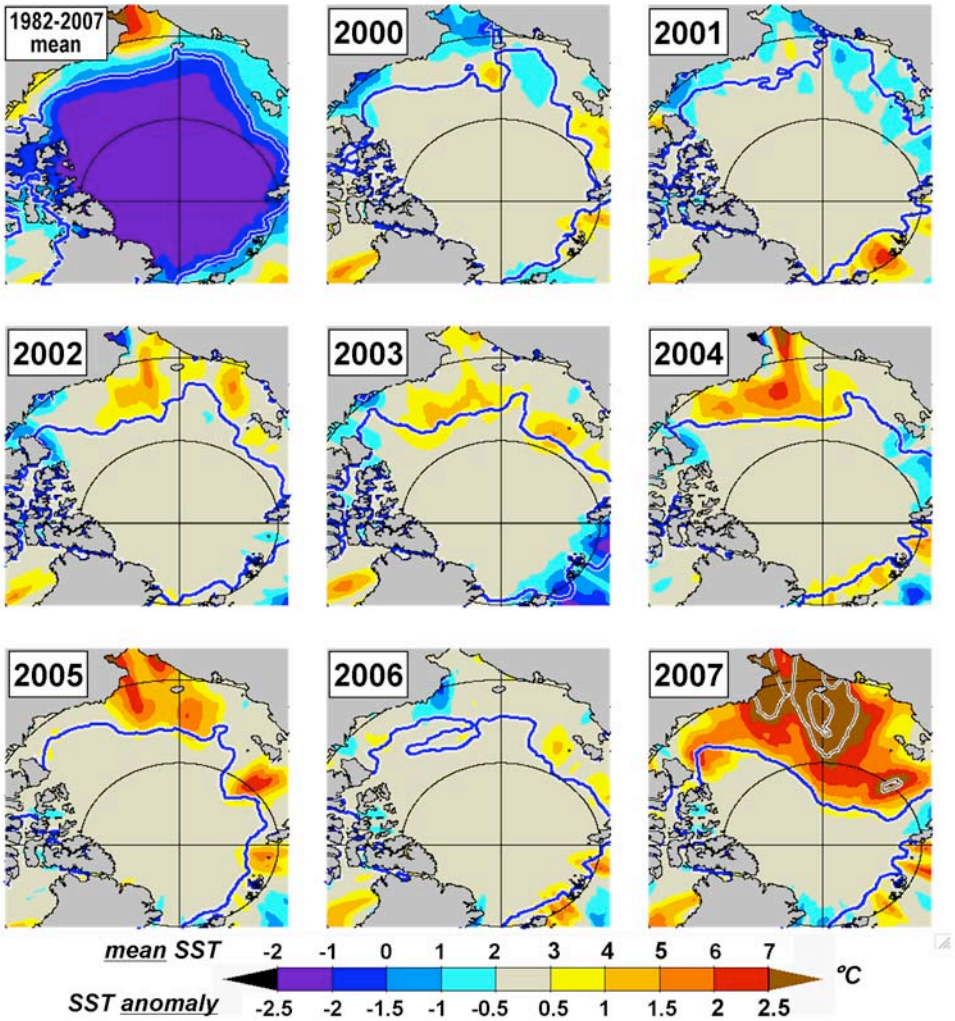

Figure 3. (top left) Mean satellite-derived summer SST [*Reynolds et al.*, 2002] and anomalies from this mean over 2000–2007, with no bias correction as in Figure 2. Latitudes 70°N and 80°N and longitudes 0°/180°E and 90°/270°E are shown. For 2007, extra contours for 3°C and 4°C are provided. Also shown is the September-mean ice edge (blue contour) from the Hadley Centre (1982–2006: http://badc.nerc.ac.uk/data/hadisst/) and from the National Centers for Environmental Prediction (2007: ftp://polar.ncep.noaa.gov/pub/cdas/).

[14] During AO+, the western Beaufort Sea region shows weakly increasing SST (Figure 1c), although OHC trends indicate a broader warming (Figure 1d). This might be explained in part by sub-surface heat advection from northward-flowing Pacific Water [*Weingartner et al.*, 2005] not resolved in the Bering Strait area by our analysis of 400 km scale trends. In fact the 50 km averaged data in Figure 1a indicates a mean northward warm advection near the Alaskan coast.

[15] Figure 2 shows time series of regional mean SST anomalies for the six marginal seas defined in Figure 1a. In situ data coverage declined dramatically since the late 1990s, partly from a lack of Russian observations and partly from lags in data synthesis into WOD'05. The Beaufort Sea time series (Figures 2a and 2b) show an anticorrelation until recent years that might have been influenced by sea ice. *Drobot and Maslanik* [2003] show that as the AO index declines, the western Beaufort Sea receives more winter sea ice from the eastern Beaufort Sea, leading to more extensive summer ice and cooler summer SSTs. The opposite conditions are found in recent years with higher AO index.

[16] Sea ice also plays a role in the ESS + Laptev Seas, where Figure 2d indicates a strong anticorrelation with springtime sea ice thickness as computed using the model of *Zhang and Rothrock* [2003]. This supports the idea that thinner/thicker sea ice at the start of the melt season leads to more/less summertime open water and thus warmer/cooler SSTs.

[17] Decadal oscillations are evident in the Kara Sea (Figure 2e) and the Barents Sea (not shown), which strongly influence the linear trends shown in Figure 1. One must thus interpret long-term trends in this region with some caution.

[18] Most regions in Figure 2 show a recent (since the late 1990s) warming. This is particularly pronounced in the Bering and Chukchi Seas (Figures 2c and 2e), which show no strong trends before this time, and in the eastern Beaufort Sea (Figure 2a) which was cooling until the early 2000s. Such wide-spread warming may be a reflection of arctic-wide sea ice retreat and the resulting increase in solar energy absorption at the ocean surface [*Perovich et al.*, 2007].

[19] Figure 3 shows satellite-derived summer-mean SST anomalies since 2000. Warm anomalies during 2002–2005

are evident north of Alaska, Bering Strait, and eastern Siberia. Maximum 2005 temperature anomalies in the northern Chukchi Sea are ~2.5°C, i.e. ~3°C above freezing since the mean in this area is about half a degree above freezing. Over a typical summer mixed layer depth of ~20 m this represents an upper ocean heat content of ~240 MJ m^{-2}, or a little more than half the 2005 solar heating of 400 MJ m^{-2} found by *Perovich et al.* [2007] in this area. This makes sense, since a significant amount of the solar energy absorption calculated by *Perovich et al.* [2007] is used to melt sea ice before it can start to warm the ocean. Temperature anomalies in 2007 are much larger than in any other year. For the northern Chukchi Sea, maximum anomalies are about double those in 2005, representing ~440 MJ m^{-2} of heat over a 20 m mixed layer.

4. Discussion

[20] Most of the Arctic Ocean peripheral seas cooled during 1930–1965 as the AO index fell, and warmed during 1965–1995 as the AO index rose. Trends in some areas (the Barents, Kara, Chukchi, and western Beaufort Seas) seem influenced at least in part by heat advection from the south. On the other hand, our data and previous work indicates that sea ice advection and summertime open water duration may be the most important factor controlling upper ocean heat trends in the ESS + Laptev and Beaufort Seas. Since the late 1990s most regions continued to warm, some at an accelerated pace which may be linked to pan-arctic sea ice retreat. However, the relative roles of sea ice retreat and ocean advection in this recent warming are not yet clear.

[21] Figure 1d shows an average increase in the upper ocean heat content of the summertime southern Chukchi and western Beaufort Seas of about 50 MJ m^{-2} $decade^{-1}$ during 1965–1995, i.e., 150 MJ m^{-2} over 30 years. *Perovich et al.* [2007] found a similar increase of 200 MJ m^{-2} in solar heating over 1979–2005 in the northern Chukchi Sea. What happens to this heat at the end of summer? Some may remain at depth below the mixed layer [*Maykut and McPhee*, 1995; *McPhee et al.*, 1998; *Steele et al.*, 2004], while the rest may be transferred to the sea ice pack by relative advection between the upper ocean and the ice. Assuming a complete transfer of heat, an upper bound may be calculated for the decrease in winter ice growth of

$$\Delta h_{ice} = (150 - 200)\text{MJ m}^{-2}/\rho_{ice}L_{ice} = 56 - 75 \text{ cm} \quad (1)$$

where sea ice density ρ_{ice} = 900 kg m^{-3} and sea ice latent heat of fusion $L_{ice} = 3 \times 10^5$ J kg^{-1} i.e., 56–75 cm less ice growth in 1995, relative to 1965. This is a significant fraction of the average ~2 m sea ice thickness in this part of the Arctic Ocean [*Zhang et al.*, 2000].

[22] If relative ocean-ice advection is small, another possibility is that the heat is simply lost to a gradually cooling atmosphere before any ice forms. This implies a delay in winter ice growth (i.e., in "fall freeze-up") of

$$\Delta t = (150 - 200)\text{MJ m}^{-2}/\rho_{air}cp_{air}ch_{aw}\Delta T_{aw}W_{10m} = 13 - 71 \text{ days} \quad (2)$$

i.e., two weeks to over two months, where air density ρ_{air} = 1.3 kg m^{-3}, air heat capacity $cp_{air} = 10^3$ J kg^{-1} °C^{-1}, air-water heat exchange coefficient $ch_{aw} = 10^{-3}$, and we assume an air-water temperature difference ΔT_{aw} = 5–10°C and 10 m elevation wind speed W_{10m} = 5–10 m s^{-1}. After this delay, the upper ocean would be cooled to the freezing point and winter sea ice growth would commence. The effect on net winter growth would probably be negligible for a delay of several weeks, but could be substantial for delays of several months.

[23] The heat transferred to the atmosphere might then be advected over other marine or terrestrial regimes. This may have played a role in recent coastal tundra ecosystem changes observed by *Chapin et al.* [1995] and others, although other factors might in fact be dominant [*Chapin et al.*, 2005]. Figure 1d shows that the western Beaufort Sea contained ~150 MJ m^{-2} more heat in 1995 relative to 1965. Assuming that this area is similar in area to the adjacent Alaskan north slope, this provides ~150 MJ m^{-2} of heat to that ecosystem, or 24–134 W m^{-2} if the air-land heat transfer rate is similar to that between the air and sea, i.e., 13–71 days as predicted by equation (2).

[24] **Acknowledgments.** This work was sponsored by the Office of Polar Programs at the National Science Foundation and by the Cryosphere Program at NASA. We thank two anonymous reviewers for critical comments.

References

Belchansky, G. I., et al. (2004), Duration of the Arctic Sea ice melt season: Regional and interannual variability, 1979–2001, *J. Clim.*, *17*, 67–80.
Chapin, F. S., et al. (1995), Responses of Arctic tndra to experimental and observed changes in climate, *Ecology*, *76*, 694–711.
Chapin, F. S., et al. (2005), Role of land-surface changes in Arctic summer warming, *Science*, *310*, 657–660.
Dickson, R., et al. (1996), Long-term coordinated changes in the convective activity of the North Atlantic, *Prog. Oceanogr.*, *38*, 241–295.
Drobot, S. D., and J. A. Maslanik (2003), Interannual variability in summer Beaufort Sea ice conditions: Relationship to winter and summer surface and atmospheric variability, *J. Geophys. Res.*, *108*(C7), 3233, doi:10.1029/2002JC001537.
Francis, J. A., and E. Hunter (2006), New insight into the disappearing arctic sea ice, *Eos Trans. AGU*, *87*(46), 509.
Gerdes, R., M. J. Karcher, F. Kauker, and U. Schauer (2003), Causes and development of repeated Arctic Ocean warming events, *Geophys. Res. Lett.*, *30*(19), 1980, doi:10.1029/2003GL018080.
Johnson, D. R., et al. (2006), *World Ocean Database, 2005 Documentation*, 163 pp., U. S. Gov. Print. Off., Washington, D. C.
Kumar, A., et al. (2003), Error characteristics of the atmospheric correction algorithms used in retrieval of sea surface temperatures from infrared satellite measurements: Global and regional aspects, *J. Atmos. Sci.*, *60*, 575–585.
Livezey, R. E., and W. Y. Chen (1983), Statistical field significance and its determination by Monte-Carlo techniques, *Mon. Weather Rev.*, *111*, 46–59.
Maslanik, J. A., et al. (1996), Recent decreases in Arctic summer ice cover and linkages to atmospheric circulation anomalies, *Geophys. Res. Lett.*, *23*, 1677–1680.
Maykut, G. A., and M. G. McPhee (1995), Solar heating of the Arctic mixed layer, *J. Geophys. Res.*, *100*, 24,691–24,703.
McPhee, M. G., et al. (1998), Freshening of the upper ocean in the Arctic: Is perennial sea ice disappearing?, *Geophys. Res. Lett.*, *25*, 1729–1732.
Ostermeier, G. M., and J. M. Wallace (2003), Trends in the North Atlantic Oscillation-Northern Hemisphere annular mode during the twentieth century, *J. Clim.*, *16*, 336–341.
Perovich, D. K., B. Light, H. Eicken, K. F. Jones, K. Runciman, and S. V. Nghiem (2007), Increasing solar heating of the Arctic Ocean and adjacent seas, 1979–2005: Attribution and role in the ice-albedo feedback, *Geophys. Res. Lett.*, *34*, L19505, doi:10.1029/2007GL031480.
Peterson, B. J., et al. (2002), Increasing river discharge to the Arctic Ocean, *Science*, *298*, 2171–2173.
Polyakov, I., et al. (2007), Observational program tracks Arctic Ocean transition to a warmer state, *Eos Trans. AGU*, *88*(40), 398.
Polyakova, E. I., A. G. Journel, I. V. Polyakov, and U. S. Bhatt (2007), Changing relationship between the North Atlantic Oscillation and key North Atlantic climate parameters, *Geophys. Res. Lett.*, *33*, L03711, doi:10.1029/2005GL024573.

Proshutinsky, A. Y., and M. A. Johnson (1997), Two circulation regimes of the wind-driven Arctic Ocean, *J. Geophys. Res.*, *102*, 12,493–12,514.

Reynolds, R. W., et al. (2002), An improved in situ and satellite SST analysis for climate, *J. Clim.*, *15*, 1609–1625.

Rigor, I. G., and J. M. Wallace (2004), Variations in the age of Arctic sea-ice and summer sea-ice extent, *Geophys. Res. Lett.*, *31*, L09401, doi:10.1029/2004GL019492.

Schauer, U., et al. (2002), Confluence and redistribution of Atlantic water in the Nansen, Amundsen and Makarov basins, *Ann. Geophys.*, *20*, 257–273.

Semiletov, I., O. Dudarev, V. Luchin, A. Charkin, K.-H. Shin, and N. Tanaka (2005), The East Siberian Sea as a transition zone between Pacific-derived waters and Arctic shelf waters, *Geophys. Res. Lett.*, *32*, L10614, doi:10.1029/2005GL022490.

Serreze, M. C., et al. (2007), Perspectives on the Arctic's shrinking sea-ice cover, *Science*, *315*, 1533–1536.

Shimada, K., T. Kamoshida, M. Itoh, S. Nishino, E. Carmack, F. McLaughlin, S. Zimmermann, and A. Proshutinsky (2006), Pacific Ocean inflow: Influence on catastrophic reduction of sea ice cover in the Arctic Ocean, *Geophys. Res. Lett.*, *33*, L08605, doi:10.1029/2005GL025624.

Steele, M., and T. Boyd (1998), Retreat of the cold halocline layer in the Arctic Ocean, *J. Geophys. Res.*, *103*, 10,419–10,435.

Steele, M., and W. Ermold (2004), Salinity trends on the Siberian shelves, *Geophys. Res. Lett.*, *31*, L24308, doi:10.1029/2004GL021302.

Steele, M., et al. (2001), PHC: A global ocean hydrography with a high-quality Arctic Ocean, *J. Clim.*, *14*, 2079–2087.

Steele, M., J. Morison, W. Ermold, I. Rigor, M. Ortmeyer, and K. Shimada (2004), Circulation of summer Pacific halocline water in the Arctic Ocean, *J. Geophys. Res.*, *109*, C02027, doi:10.1029/2003JC002009.

Stroeve, J., et al. (2006), Recent changes in the Arctic melt season, *Ann. Glaciol.*, *44*, 367–374.

Weingartner, T., et al. (2005), Circulation on the north central Chukchi Sea shelf, *Deep Sea Res., Part II*, *52*, 3150–3174.

Woodgate, R. A., K. Aagaard, and T. J. Weingartner (2006), Interannual changes in the Bering Strait fluxes of volume, heat and freshwater between 1991 and 2004, *Geophys. Res. Lett.*, *33*, L15609, doi:10.1029/2006GL026931.

Zhang, J. (2005), Warming of the arctic ice-ocean system is faster than the global average since the 1960s, *Geophys. Res. Lett.*, *32*, L19602, doi:10.1029/2005GL024216.

Zhang, J. L., and D. A. Rothrock (2003), Modeling global sea ice with a thickness and enthalpy distribution model in generalized curvilinear coordinates, *Mon. Weather Rev.*, *131*, 845–861.

Zhang, J., et al. (1998), Warming of the Arctic Ocean by a strengthened Atlantic inflow: model results, *Geophys. Res. Lett.*, *25*, 1745–1748. (Correction, *Geophys. Res. Lett.*, *25*, 3541, 1998.)

Zhang, J. L., et al. (2000), Recent changes in Arctic sea ice: The interplay between ice dynamics and thermodynamics, *J. Clim.*, *13*, 3099–3114.

W. Ermold, M. Steele, and J. Zhang, Polar Science Center, Applied Physics Laboratory, University of Washington, Seattle, WA 98105, USA. (mas@apl.washington.edu)